

AN ABSTRACT OF THE THESIS OF

Shelby R. Young _____ for the Master of Science
(name of student) (degree)

In Forensic Science _____ presented on
March 19th, 2020

Title:

Testing the Use of Attenuated Total Reflectance Fourier Transform Infrared Spectroscopy for
Differentiating Forensic Soil Samples in Kansas

Thesis Chair: Dr. Melissa Bailey

Abstract approved: _____
(Thesis Advisor Signature)

This experiment explored the feasibility of using attenuated total reflectance-Fourier transform infrared radiation (ATR-FTIR) as a preliminary method to identify and differentiate forensic soil samples in Lyon County, Kansas. Current methods used by soil scientists such as polarized light microscopy, inductively coupled plasma- mass spectroscopy (ICP-MS), atomic fluorescence spectroscopy, x-ray fluorescence spectroscopy, and scanning electron microscopy- energy dispersive x-ray (SEM-EDX) are time consuming, destructive, costly, and are not available in all forensic laboratories. ATR-FTIR is nondestructive and is commonly used in forensic laboratories for trace evidence analysis. One hundred surface soil samples and one hundred samples obtained 15.24 cm (6 in) below the surface were collected in five diverse locations of the Ross Natural History Reservation (Ross) located in Lyon County, Kansas. A blind study was conducted with twenty-five additional soil samples from either the surface or subsurface from unknown locations of the Ross. All soil samples were dried, homogenized, and analyzed using ATR-FTIR. Visual comparisons of the data displayed a substantial spectral difference between both layers of soil and minimal observable differences for the areas where soils were sampled. The ATR-FTIR OPUS software correctly identified the origin of 92% of the blind samples. Principal component analysis (PCA) was utilized to highlight small variations and identified the origin of 100% of the blind samples. Results from this study demonstrated that ATR-FTIR can be used as a preliminary screening tool in forensic soil analyses and may offer significant advantages over other, more costly, methods.

Keywords: Forensic Soil Analysis, Infrared Spectroscopy, ATR-FTIR

TESTING THE USE OF ATTENUATED TOTAL REFLECTANCE FOURIER TRANSFORM
INFRARED SPECTROSCOPY FOR DIFFERENTIATING FORENSIC SOIL SAMPLES IN
KANSAS

A Thesis

Presented to

The Department of Biological Sciences

EMPORIA STATE UNIVERSITY

In Partial Fulfillment

Of the Requirements for the Degree

Master of Science in Forensic Science, Chemistry Concentration

By

Shelby Renee Young

May 2020



Approved by the Department Chair



Committee Member



Committee Member



Committee Member

Dean of the Graduate School and Distance Education

ACKNOWLEDGMENTS

My deepest thanks to my thesis chair, Dr. Melissa Bailey, my committee members, Dr. Richard Sleezer and Jeremiah Morris, to my number 1 supporter, Nathan Collins, and my parents, Elmer and Darbie Young.

STYLE MANUAL

This thesis was written according to the guidelines of the Journal of the American Society of Trace Evidence Examiners (JASTEE).

TABLE OF CONTENTS

	<u>Page</u>
ACKNOWLEDGEMENTS.....	iii
TABLE OF CONTENTS	v
LIST OF TABLES	vi
LIST OF FIGURES	vii
<u>CHAPTER</u>	
1 INTRODUCTION.....	1
2 METHODS AND MATERIALS	4
Sample Collection	4
ATR Analysis.....	5
Principal Component Analysis.....	5
3 RESULTS AND DISCUSSION	7
Soil Characterization	7
Soil Differentiation.....	9
4 CONCLUSION.....	12
REFERENCES	14
Permission to Copy Page.....	35

LIST OF TABLES

<u>Table</u>		<u>Page</u>
1	Results of OPUS Spectra Search and PCA Compared to Actual Soil Origin	32
2	Proposed Assignments for Peak Positions in the ATR-FTIR Spectra	33
3	PCA Eigenvalues and Their Contribution to the Correlations.....	34

LIST OF FIGURES

<u>Figure</u>		<u>Page</u>
1	Web Soil Survey of The Ross Natural History Reservation.....	17
2	GPS Coordinate Map.....	18
3	Area 1 ATR-FTIR Spectra.....	19
4	Area 2 ATR-FTIR Spectra.....	20
5	Area 3 ATR-FTIR Spectra.....	21
6	Area 4 ATR-FTIR Spectra.....	22
7	Area 5 ATR-FTIR Spectra.....	23
8	Area 1 ATR-FTIR Layer Spectra.....	24
9	Area 2 ATR-FTIR Layer Spectra.....	25
10	Area 3 ATR-FTIR Layer Spectra.....	26
11	Area 4 ATR-FTIR Layer Spectra.....	27
12	Area 5 ATR-FTIR Layer Spectra.....	28
13	Unknown Sample 25 Spectra Air Dried Compared to Oven Dried	29
14	PCA Ordination Plot displaying PC1 and PC6 for Soil Area.....	30
15	PCA Ordination Plot displaying PC1 and PC2 for Soil Layer	31

Chapter 1

INTRODUCTION

There are many analytical methods used for soil analysis, including polarized light microscopy, inductively coupled plasma mass spectroscopy (ICP-MS), atomic fluorescence spectroscopy, X-ray fluorescence spectroscopy, and scanning electron microscopy-energy dispersive X-ray spectroscopy [1]. Unfortunately, these methods come with many disadvantages in the field of forensic science. They can be time consuming, destructive, costly, and are not available at all forensic laboratories [1, 2]. In some laboratories, soil analysis is not performed routinely or at all due to these challenges [2]. The lack of soil analyses is unfortunate, because the characterization and differentiation of soils is a powerful tool in trace evidence and may be useful in determining the origin of a crime or linking a crime scene to a suspect or victim [3]. Soil has many complex biological, chemical, physical, and mineralogical properties that vary by region and constantly change with time [4]. This variation in soil properties is commonly explained based on five factors that affect soil formation: climate, organism, relief, parent material, and time [4]. Differences in temperature and rate of precipitation across various climates profoundly influences the chemical and physical processes of soil formation in a given area [5]. The activities of organisms (plants, animals and even bacteria) within and above the soil are influenced by climate and modify the soil's composition by affecting the accumulation of organic matter within the upper soil and influencing rates of erosion [5]. Differences in topography or relief (slope steepness, slope shape, and slope aspect) can influence rates of erosion and either increase or decrease the effects of climatic variability [5]. Parent material for soil formation can be the weathering products of underlying rocks (residuum), or it can originate from the weathering of geologic materials that have been transported and deposited by water,

wind or ice [5]. The formation of soil is also affected by the amount of time it takes for the weathering of rock, translocation of materials within soil profiles, and accumulation of organic matter in soil [5]. The combination and complexity of these five factors form soil that is unique to its own region or landscape. Soil is also composed of air, water, minerals, and organic material in varying proportions [5]. The combination of various minerals and organic particles found in soil are unique to their setting and identifying these differences is crucial in forensic applications [4]. According to the Locard Exchange Principle, when two surfaces come into contact, there is potential for shared transfer of material between them [3]. Therefore, soil can be observed on the surface of a suspect's shoes, clothing, vehicle, or tools related to a crime [3]. Recently, interest in forensic soil analysis has increased due to the contribution of soil evidence in high profile cases [2, 6]; however, the characterization of soil is complex. Consequently, finding quick, user friendly, and non-destructive methods is of high interest [7].

One instrument common to many forensic laboratories is attenuated total reflectance-Fourier transform infrared spectroscopy (ATR-FTIR) [1]. This instrument is used frequently for chemical analysis of several types of trace evidence such as paint [8], paper [9], tape [10], and fibers [7] with minimal sample preparation. Other major advantages to ATR-FTIR are that this method is nondestructive and requires only a small amount of the sample, which is particularly advantageous in cases where evidence is limited [2]. The spectra produced from the ATR-FTIR analysis can assist in identifying the composition of both the organic and inorganic components of soil [1, 6]. This range of applicability is useful for characterizing the biological material present in soil organic matter (SOM) [11], primary minerals such as quartz, and secondary minerals such as calcite, gypsum, and malachite commonly found in soils [5]. The presence and abundance of these minerals, as well as unique biological materials such as pollen, are some of

the main attributes that link a soil to a region [5]. ATR-FTIR uses a high refractive index ATR crystal (such as a diamond) to internally reflect infrared radiation (IR) when it interacts with a sample [12]. Absorption of IR by the sample reduces the initial intensity [12]. These changes in the infrared light are transformed into a frequency domain signal by Fourier analysis and produce IR spectra [12]. These spectra can be analyzed by identifying peaks associated with specific vibrational modes of chemical bonds [12]. Small spectral differences are not always easily observable and are better visualized utilizing multivariate analysis [13]. Many studies have used ATR-FTIR paired with Principle Component Analysis (PCA) to highlight potential differences in spectral data [1, 7, 9, 13, 14]. PCA condenses the dimensions of large data sets into principal components that retain the variation in the data while reducing the dimensions of the dataset into orthogonal axes, each of which represents multiple variables [20]. This study aims to apply PCA to the spectra produced from ATR-FTIR for this purpose.

Few studies have examined the forensic application of ATR-FTIR for soil analysis. Most studies have focused on using ATR-FTIR to distinguish soils from widely spaced geographic areas [1, 2]. At the time of this research, no studies have tested the use of ATR-FTIR with a blind study or within a considerably smaller region. This experiment aimed to investigate the discriminatory power of ATR-FTIR by utilizing a small region within Kansas and performing a blind study with unknown samples from that same study area. Furthermore, the potential of ATR-FTIR was demonstrated for forensic soil analysis and emphasized for the laboratories in regions where resources are limited.

Chapter 2

METHODS AND MATERIALS

Sample Collection

Five diverse areas within the 200 acre plot of the Ross Natural History Reservation (Ross) located in Lyon County, Kansas were selected utilizing a web soil survey map produced by the United States Department of Agriculture Natural Resources Conservation Service (USDA NRCS) (Figure 1) [15]. The following map units were chosen for sampling; 4744 Labette-Dwight complex (area 1), 8777 Kenoma silty clay loam (area 2), 4590 Clime-Sogn complex (area 3), 7306 Martin silty clay (area 4) and 4740 Labette silty clay loam (area 5). A Garmin eTREX GPS unit was used to find the location of each soil map area. Twenty collection sites within each area were randomly selected by blindly throwing a disk from a central location within the area to avoid sample selection bias. Numbered flags were used to designate the spot where the frisbee landed. The GPS coordinates for every flag were recorded (Figure 2). A 30.48 cm (12 in) soil probe was utilized to collect soil at the base of each flag. The soil core was split in half to represent surface and subsurface soil, wrapped in aluminum foil, labeled, and stored in a cooler until all samples were collected. The soil was air dried for three months to avoid oversaturation of the ATR-FTIR detector by moisture. Samples were homogenized with a mortar and pestle, blended until the soil was a fine powder, and then stored in 50 mL centrifuge tubes. All equipment was thoroughly cleaned between samples to prevent contamination from the previous soil. Five additional (blind) samples were randomly selected from each area and prepared by an assistant in the same fashion as the original samples. A number between 1 and 25 and layer of soil were randomly assigned to every sample by the assistant. A total of 200 known samples and 25 blind samples were collected and prepared using these methods.

ATR Analysis

The soil samples were analyzed using a Bruker Optics FTIR spectrometer ALPHA with a diamond ATR module. Instrument parameters were set to 4000-400 cm^{-1} range, 4 cm^{-1} resolution, 24 background scans, and 24 sample scans. A 10-15 milligram scoop was utilized to measure approximately the same amount of soil for all samples. The homogenized soil was placed directly on the detection window to be pressed onto the diamond ATR crystal. Consistent pressure between the sample and the handle of the ATR-FTIR was maintained to avoid variances due to pressure. Normalization, atmospheric compensation, and background correction were applied to all spectra. Five different spectra were collected for each sample to assess the variability of the spectra within each sample. The sample was removed, a background scan was run, and a new aliquot of the same sample was added to achieve five different spectra per sample. An operational qualification test assessing resolution, sensitivity, and wavenumber accuracy was completed and passed before beginning this experiment. A performance qualification test assessing signal to noise, interferogram peaks, and wavelength accuracy, was completed and passed before scanning any samples on the ATR-FTIR each day of analysis. A library containing all the spectra produced from areas one through five was created utilizing OPUS version 8.1 software. A spectra search was performed to compare the unknown blind samples to the spectra obtained from the library (Table 1).

Principal Component Analysis

Principal Component Analysis (PCA) and graphs were performed in program R [16] using packages *vegan* [17], *ggplot2* [18], and *wesanderson* [19]. The objective was to determine the discriminatory power of ATR-FTIR for forensic soil examinations. Prior to analysis, the five samples within each collection site were averaged to remove pseudo replication for a total of 225

spectra. No arch effect was detected based on a Detrended Correspondence Analysis (DCA, axis length < 4 , decorana command in R), indicating that PCA is acceptable for these data [21]. The PCA produced 217 principal components that represented the variation present in this spectral data set. A broken stick model and the Kaiser-Guttman test suggest that the first 11 axes were interpretable [22]. Based on graphical interpretability, results from axes 1, 2, and 6 are presented.

Chapter 3

RESULTS AND DISCUSSION

Soil Characterization

ATR-FTIR spectroscopy can be used to analyze both the organic and inorganic components of soil. Cellulose, lignin, polysaccharides, and many other components of plant material have characteristic vibrational modes in the mid-range of infrared radiation (4000-400 cm^{-1}) [23]. This is also true for minerals commonly found in soil such as calcite, quartz, kaolinite, and many more [24]. Table 2 displays the main components of soil present in this study with assigned absorption bands. These proposed assignments were made from comparisons of reliable IR spectra from previous research [23, 25-31]. According to scientific literature, organic material such as lignin and cellulose display a broad peak at approximately 3400-3300 cm^{-1} representing O-H stretching in hydroxyl groups [23, 28]. Another peak at approximately 1650-1600 cm^{-1} is significant for aromatic C=C stretching or C-O stretching of lignin, aliphatic carboxylates, and other aromatic compounds depending on the peak intensity and shape [23, 28]. However, these peak locations are also reported in literature to be due to water hydration [30, 31]. Figures 8-12 display the varying absorbances in the peaks around 3400 and 1630 cm^{-1} for both layers of soil collected for all five areas. A broad peak and a short broad peak are present at approximately 3394 and 1632 cm^{-1} respectively. To determine if these peaks were caused by the presence of water, a sample was weighed (146.7 g), oven-dried at 100°C overnight, and weighed again (142.9 g) according to a sample preparation technique described in a standard loss on ignition organic carbon standard operating procedure [32]. The sample that dried overnight lost 3.8 g of mass, indicating that it still contained a significant amount of water after air drying. To determine the spectral effect of oven drying, the sample was reanalyzed via ATR-FTIR. Figure

13 displays the difference between the air dried and oven dried sample. The peaks associated with O-H stretching 3400 cm^{-1} and H-O-H deformation 1632 cm^{-1} are significantly reduced in the oven dried sample. This observation indicates that the ability to access organic content in the present soil samples is very limited if possible at all due to the presence of water. The difference in absorbance between layers for these peaks may indicate a difference in the water retention characteristics of the soils sampled [33].

Identifying whether soil evidence originates from the surface or subsurface is crucial for revealing whether evidence was buried or transferred from the topsoil. The only exception for this phenomenon was found in area 3. It was difficult to see a clear difference between the subsurface and surface of the soil found in area 3. This could be due to the soil composition. Area 3 is composed of Clime-Sogn soil. The Sogn series of soil is characterized as shallow, loamy, and formed from limestone [34]. Limestone is primarily made up of the calcium carbonate mineral calcite. [27]. Spectral peaks for calcite were found in area 3. These spectral peaks are positioned at approximately 1422 and 872 cm^{-1} (Figure 10). Literature sources agree that C-O and CO^{-3} vibrational modes of carbonate typically occur at 1440 - 1395 and 900 - 825 cm^{-1} respectively [27]. The calcite polymorph of calcium carbonate is differentiated from others by the location of the lower peak [27]. This study has found that the subsurface soil for most areas display higher absorbances for the peaks of water hydration. This is most likely due to increases in phyllosilicate clays with depth that have greater water absorbance properties [5]. However, the samples containing calcite in area 3 displayed the lowest absorbances for water retention. The lower water absorbency in area 3 soils is most likely due to the shallow and rocky composition of the soil. Therefore, it was difficult to decipher what layer of soil area 3 samples originated from.

Previous studies have indicated characteristic peaks for the primary mineral, quartz, at approximately 1,085, 800, 780, 695, 514 and 462 cm^{-1} [26]. These peaks were consistently observed in this study. Figures 3-7 display these quartz and similar silicate peaks generally around 1100, 795, 777, and 692 cm^{-1} . Other lower peaks were visible, but the accuracy at longer wavelengths is not guaranteed due to the ATR crystal. Therefore, only peaks above 525 cm^{-1} were included in these analyses. The 1100 cm^{-1} band corresponds to asymmetric Si-O stretching. The split peaks at 795 and 777 cm^{-1} represent Si-O-Si symmetrical stretching, and the 692 cm^{-1} band indicates Si-O bending [26].

Another mineral commonly found in soil is kaolinite, a secondary aluminum silicate mineral. Kaolinite displays specific vibrational modes at approximately 3694, 3650, 3620, 1114, 1032, 1010, 936, 912, 790, 752, 693, 537, 468, and 430 cm^{-1} according to literature [25]. The bands at approximately 3695, 3623, 1100, 995, 911, 795, and 692 in the spectra of this study indicate the presence of kaolinite in these soil samples. Many of these bands are similar to quartz, because both of these minerals are silicates with Si-O stretching vibrational modes. Kaolinite's chemical formula is $\text{Al}_2\text{Si}_2\text{O}_5(\text{OH})_4$. Therefore, there are additional bands such as 3695 and 3623 cm^{-1} for OH stretching of hydroxyl groups and 911 cm^{-1} for O-H bending. These peaks have the relative wave number location, shape, and intensity unique to kaolinite compared to other silicate minerals [25]. Other bands such as 995 and 795 cm^{-1} represent in-plane Si-O stretching and symmetrical Si-O stretching respectively [25, 26]. Other minerals may be present but are not easily separated and identified in the spectra. All areas of soil collection display varying amounts of absorption for these minerals.

Soil Differentiation

The soil collected within the Ross displays similar peaks with the addition of two calcite peaks for several samples found within area 3. However, similar spectra make it difficult for qualitative analysis. According to Table 1, only 68% of the top hits from the spectra search were correct in identifying the origin of the blind samples. Of the top five hits from the spectra search, 92% of the blind samples' areas of origin were correctly identified. Visual comparisons of the spectra may be acceptable for investigative leads with this method. However, it could also cause inaccurate results. This study shows that samples that contain similar chemical composition may have the same peaks in FTIR spectra with only varying intensities. Cases involving many samples, as this study did, make visual comparisons very time consuming and difficult to differentiate. Therefore, multivariate analysis is advantageous to attain quicker results and consistent differentiation. PCA is a quicker, reliable, and more accurate approach to identifying small spectral differences [14]. There are many different software packages capable of multivariate analysis including R, SPSS, MATLAB, Minitab, Excel XLSTAT that are easily available to forensic scientists for this purpose [20].

Initially, it was found that 90% of the variation in the data set was shown by the first eleven principal components (PCs). However, results of the first six PCs were selected to review because they represent 85% of the variation. The results from the PCA are displayed in Table 3. Figure 15 shows the ordination plot for PC1 and PC2 of the variation between the soil layers. Two distinct groupings were identified with sub-surface soil on the left and surface soil on the right of Figure 15. PC1 and PC2 represent 49% and 15% of the overall variance in the dataset respectively. Given the massively differing intensities for the 3394 cm^{-1} band, it was suggested that PC1 was strongly influenced by the O-H stretching due to the presence of water. The other peak that was significantly impacted by the soil layer water retention was at approximately 1630

cm^{-1} . This finding implies that PC2 was substantially affected by H-O-H deformation due to moisture content. The blind samples were overlain on top of the ordination plot to determine their original source location. This method resulted in 100% of the blind samples being correctly matched to their respective layer of soil.

Figure 14 shows the ordination plot for PC1 and PC6 of the variation between the soil areas. Both layers of soil were combined for this PCA, so that only five locations would be displayed. It was established that PC1 represents the variation of the 3394 cm^{-1} vibrational band. However, PC6 only explains 3% of the variance and was more difficult to detect the source of variation. Figure 14 displays that area 4 was almost entirely separated from the other groupings. This finding indicated that the subtle differences in all the areas were enhanced in area 4. In the same figure, area 5 was split into almost two complete groupings on opposite sides of PC1. This indicated the PC6 variation of area 5 was split between the layers. The only peak consistent with this phenomenon was found at approximately 1100 cm^{-1} . This implied that PC6 may be influenced by Si-O stretching of various silicate minerals such as quartz and kaolinite. The blind samples were overlain on top of the ordination plot to visualize the areas of soil the samples originated from. This method resulted in 100% of the blind samples being correctly matched to their respective area of origin.

Chapter 4

CONCLUSIONS

In the present study, 100 surface and 100 sub-surface soil samples from five diverse areas of the Ross Natural History Reservation in Lyon County, Kansas were characterized and differentiated using ATR-FTIR spectroscopy paired with the multivariate technique, principal component analysis. A blind study was conducted to determine the origin of 25 unknown soil samples. The ability of ATR-FTIR to determine the area of origin of unknown soil samples was verified with 92% accuracy via OPUS SpectraSearch and 100% accuracy via PCA. This conclusion suggests that this technique has the potential to be extremely useful for quick determination of whether soil evidence is consistent with soil found from a crime scene or suspect. This study was the first to conduct a blind study and show that ATR-FTIR can be used to determine the origin of blind samples within a considerably small region of less than 200 acres

This research has the potential to assist in developing a soil database or updating chemical information of soil map units [35, 36]. Other future considerations include assessing the effect of time on the variation of soil or collecting soil from greater depths. A limitation of this method is that it was unable to determine the chemical composition of molecules without dipole moments [9]. Additionally, some functional groups produce broad peaks that overlap producing an incomplete assessment of the chemical makeup [9]. The presence of broad peaks due to moisture content also has the potential to overlap crucial peaks for a complete assessment of the chemical composition. This study was unable to access to the ability of ATR-FTIR to characterize or differentiate the organic portion of soil because of the presence of water. One recommendation from this study is that soil samples to be used for ATR-FTIR should be oven-dried before analysis.

ATR-FTIR has the potential to be used with quick and nondestructive techniques such as microspectrophotometry (MSP) and X-ray fluorescence spectroscopy (XRF) to determine color and elemental information respectively [37]. Use of these methods would be advantageous to the forensic science community by increasing soil comparisons as a routine form of trace evidence. These instruments are found in almost all forensic laboratories and produce quick turnaround times that will create investigative leads. Furthermore, ATR-FTIR with PCA is a reliable, efficient, and non-destructive preliminary screening method for forensic soil evidence that is capable of detecting differences in chemical composition.

REFERENCES

1. Chauhan, R., Kumar, R., & Sharma, V. (2018). Soil forensics: A spectroscopic examination of trace evidence. *Microchemical Journal*, 139, 74-84. doi:10.1016/j.microc.2018.02.020
2. Woods, B., Lennard, C., Kirkbride, K. P., & Robertson, J. (2016). Reinstating Soil Examination as a Trace Evidence Sub-discipline. *Soil in Criminal and Environmental Forensics*, 107–120. doi: 10.1007/978-3-319-33115-7_7
3. Fitzpatrick, R. W. (2013). Soil: Forensic Analysis. *Wiley Encyclopedia of Forensic Science*. doi: 10.1002/9780470061589.fsa096
4. Fitzpatrick, R. (2008). Nature, Distribution, and Origin of Soil Materials in the Forensic Comparison of Soils. *Soil Analysis in Forensic Taphonomy*, 1–28. doi: 10.1201/9781420069921.ch1
5. Brady, N. C., & Weil, R. R. (2017). *The Nature and Properties of Soils* (15th ed.). Pearson.
6. Woods, B., Lennard, C., Kirkbride, K. P., & Robertson, J. (2014). Soil examination for a forensic trace evidence laboratory—Part 1: Spectroscopic techniques. *Forensic Science International*, 245, 187–194. doi: 10.1016/j.forsciint.2014.08.009
7. Peets, P., Leito, I., Pelt, J., & Vahur, S. (2017). Identification and classification of textile fibres using ATR-FT-IR spectroscopy with chemometric methods. *Spectrochimica Acta Part A: Molecular and Biomolecular Spectroscopy*, 173, 175–181. doi: 10.1016/j.saa.2016.09.007
8. Spring, M., Ricci, C., Peggie, D. A., & Kazarian, S. G. (2008). ATR-FTIR imaging for the analysis of organic materials in paint cross sections: case studies on paint samples from the National Gallery, London. *Analytical and Bioanalytical Chemistry*, 392(1-2), 37–45. doi: 10.1007/s00216-008-2092-y
9. Kumar, R., Kumar, V., & Sharma, V. (2017). Fourier transform infrared spectroscopy and chemometrics for the characterization and discrimination of writing/photocopier paper types: Application in forensic document examinations. *Spectrochimica Acta Part A: Molecular and Biomolecular Spectroscopy*, 170, 19–28. doi: 10.1016/j.saa.2016.06.042
10. Goodpaster, J. V., Sturdevant, A. B., Andrews, K. L., Briley, E. M., & Brun-Conti, L. (2009). Identification and Comparison of Electrical Tapes Using Instrumental and Statistical Techniques: II. Organic Composition of the Tape Backing and Adhesive. *Journal of Forensic Sciences*, 54(2), 328–338. doi: 10.1111/j.1556-4029.2008.00969.x
11. Tan, K. H. (2011). *Principles of Soil Chemistry* (4th ed.). Boca Raton, FL: CTC Press Taylor & Francis Group.
12. Zhang, J., Li, B., Wang, Q., Wei, X., Feng, W., Chen, Y., ... Wang, Z. (2017). Application of Fourier transform infrared spectroscopy with chemometrics on postmortem interval estimation based on pericardial fluids. *Scientific Reports*, 7(1). doi: 10.1038/s41598-017-18228-7
13. Smith, M. J., Holmes-Smith, A. S., & Lennard, F. (2019). Development of non-destructive methodology using ATR-FTIR with PCA to differentiate between historical

- Pacific barkcloth. *Journal of Cultural Heritage*, 39, 32–41. doi: 10.1016/j.culher.2019.03.006
14. Sharma, V., Bhardwaj, S., & Kumar, R. (2019). On the spectroscopic investigation of Kohl stains via ATR-FTIR and multivariate analysis: Application in forensic trace evidence. *Vibrational Spectroscopy*, 101, 81–91. doi: 10.1016/j.vibspec.2019.02.006
 15. USDA NRCS. (n.d.). Web Soil Survey. Retrieved from <https://websoilsurvey.sc.egov.usda.gov/>
 16. R Core Team (2019). R: A language and environment for statistical computing. R Foundation for Statistical Computing, Vienna, Austria. URL <https://www.R-project.org/>.
 17. Jari Oksanen, F. Guillaume Blanchet, Michael Friendly, Roeland Kindt, Pierre Legendre, Dan McGlinn, Peter R. Minchin, R. B. O'Hara, Gavin L. Simpson, Peter Solymos, M. Henry H. Stevens, Eduard Szoecs and Helene Wagner (2019). *vegan: Community Ecology Package*. R package version 2.5-6. <https://CRAN.R-project.org/package=vegan>
 18. H. Wickham. *ggplot2: Elegant Graphics for Data Analysis*. Springer-Verlag New York, 2016.
 19. Karthik Ram and Hadley Wickham (2018). *wesanderson: A Wes Anderson Palette Generator*. R package version 0.3.6. <https://CRAN.R-project.org/package=wesanderson>
 20. Kumar, R., & Sharma, V. (2018). Chemometrics in forensic science. *TrAC Trends in Analytical Chemistry*, 105, 191–201. doi: 10.1016/j.trac.2018.05.010
 21. Legendre, P., & Birks, H. J. B. (2012). From Classical to Canonical Ordination. *Tracking Environmental Change Using Lake Sediments Developments in Paleoenvironmental Research*, 201–248. doi: 10.1007/978-94-007-2745-8_8
 22. Jackson, J. E. (2003). *A Users Guide to Principal Components*. Hoboken, NJ: Wiley-Interscience.
 23. Artz, R. R., Chapman, S. J., Robertson, A. J., Potts, J. M., Laggoun-Défarge, F., Gogo, S., ... Francez, A.-J. (2008). FTIR spectroscopy can be used as a screening tool for organic matter quality in regenerating cutover peatlands. *Soil Biology and Biochemistry*, 40(2), 515–527. doi: 10.1016/j.soilbio.2007.09.019
 24. Xu, Z., Cornilsen, B. C., Popko, D. C., Pennington, W. D., Wood, J. R., & Hwang, J.-Y. (2001). Quantitative Mineral Analysis by FTIR Spectroscopy. *Journal of Vibrational Spectroscopy*, 5(6).
 25. Vaculíková, L., Plevová, E., Vallová, S., & Koutník, I. (2010). Characterization and differentiation of kaolinites from selected Czech deposits using infrared spectroscopy and differential thermal analysis. *Acta Geodynamica Et Geomaterialia*, 8(1), 59–67.
 26. Ojima, J. (2003). Determining of Crystalline Silica in Respirable Dust Samples by Infrared Spectrophotometry in the Presence of Interferences. *Journal of Occupational Health*, 45(2), 94–103. doi: 10.1539/joh.45.94
 27. Gunasekaran, S., Anbalagan, G., & Pandi, S. (2006). Raman and infrared spectra of carbonates of calcite structure. *Journal of Raman Spectroscopy*, 37(9), 892–899. doi: 10.1002/jrs.1518
 28. Bernier, M.-H., Levy, G. J., Fine, P., & Borisover, M. (2013). Organic matter composition in soils irrigated with treated wastewater: FT-IR spectroscopic analysis of bulk soil samples. *Geoderma*, 209-210, 233–240. doi: 10.1016/j.geoderma.2013.06.017
 29. Ellerbrock, R. H., & Gerke, H. H. (2004). Characterizing organic matter of soil aggregate coatings and biopores by Fourier transform infrared spectroscopy. *European Journal of Soil Science*, 55(2), 219–228. doi: 10.1046/j.1365-2389.2004.00593.x

30. Salil, M. S., Shrivastava, J. P., & Pattanayak, S. K. (1997). Similarities in the mineralogical and geochemical attributes of detrital clays of Maastrichtian Lameta Beds and weathered Deccan basalt, Central India. *Chemical Geology*, 136(1-2), 25–32. doi: 10.1016/s0009-2541(96)00128-3
31. Anbalagan, G., Prabakaran, A. R., & Gunasekaran, S. (2010). Spectroscopic characterization of indian standard sand. *Journal of Applied Spectroscopy*, 77(1), 86–94. doi: 10.1007/s10812-010-9297-5
32. Myrbo, A., Plank, C., Coleman, J., Shane, L., & Graber, D. (2013, November 11). Loss-on-Ignition Standard Operating Procedure. Retrieved March 28, 2020, from <http://lrc.geo.umn.edu/laccore/assets/pdf/sops/loi.pdf>
33. Janik, L. J., Merry, R. H., Forrester, S. T., Lanyon, D. M., & Rawson, A. (2007). Rapid Prediction of Soil Water Retention using Mid Infrared Spectroscopy. *Soil Science Society of America Journal*, 71(2), 507–514. doi: 10.2136/sssaj2005.0391
34. NRCS. (n.d.). NRCS Official Soil Series Description. Retrieved from <https://soilseries.sc.egov.usda.gov/osdname.aspx>
35. Menchaca, P. R., Graham, R. C., & Younglove, T. (2018). Developing and Testing a Soil Property Database for Forensic Applications in Southern California. *Journal of Forensic Sciences*, 63(4), 1043–1052. doi: 10.1111/1556-4029.13723
36. Suarez, M. D., Southard, R. J., & Parikh, S. J. (2015). Understanding Variations of Soil Mapping Units and Associated Data for Forensic Science. *Journal of Forensic Sciences*, 60(4), 894–905. doi: 10.1111/1556-4029.12762
37. Woods, B., Lennard, C., Kirkbride, K. P., & Robertson, J. (2016). Soil examination for a forensic trace evidence laboratory—Part 3: A proposed protocol for the effective triage and management of soil examinations. *Forensic Science International*, 262, 46–55. doi: 10.1016/j.forsciint.2016.02.034



Figure 1: Web Soil Survey of The Ross Natural History Reservation Provided by the United States Department of Agriculture Natural Resources Conservation Service

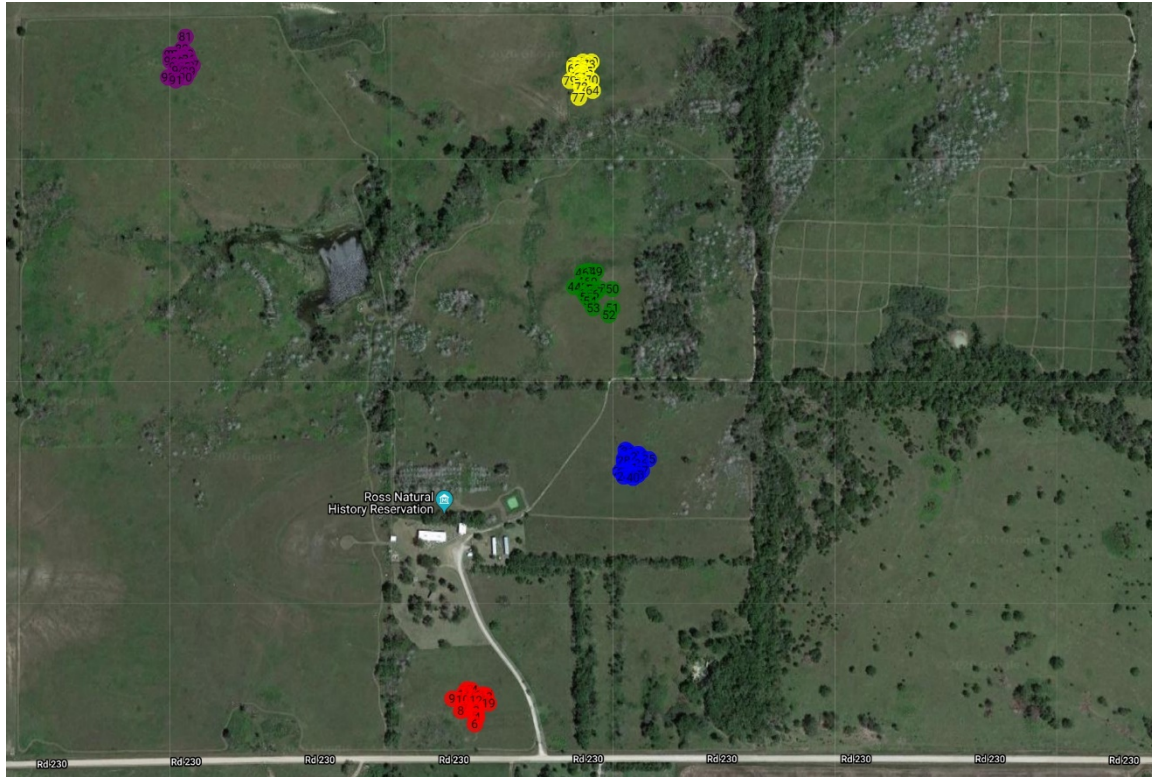


Figure 2: GPS Coordinate Map of Area 1 (red), Area 2 (blue), Area 3 (green), Area 4 (yellow), and Area 5 (purple)

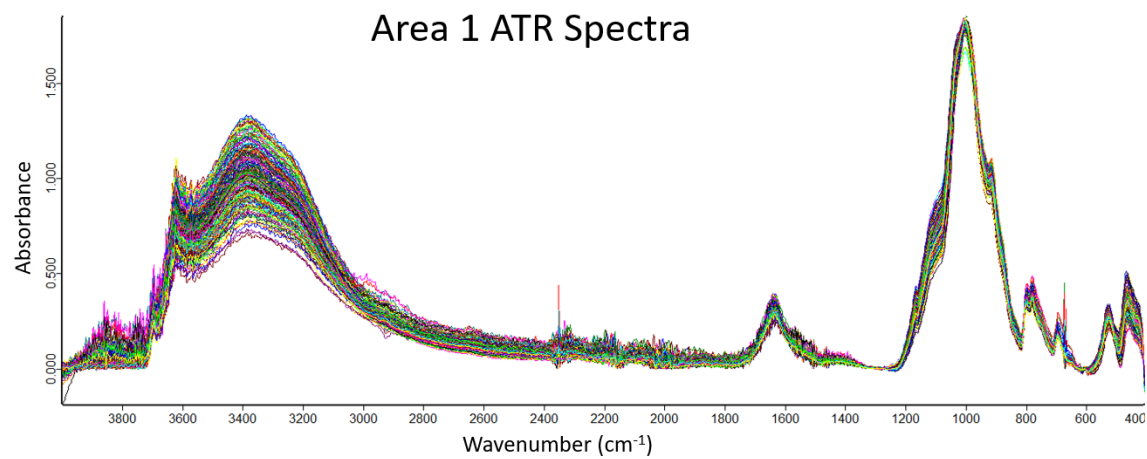


Figure 3: Area 1 ATR-FTIR Spectra Consisting of 20 Surface Samples and 20 Sub-surface Samples with 5 Replicates Each

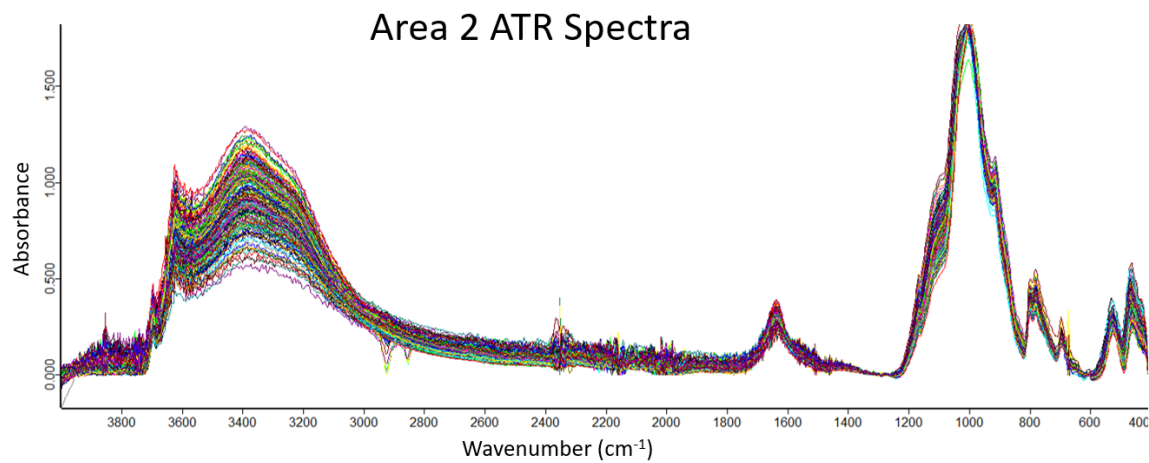


Figure 4: Area 2 ATR-FTIR Spectra Consisting of 20 Surface Samples and 20 Sub-surface Samples with 5 Replicates Each

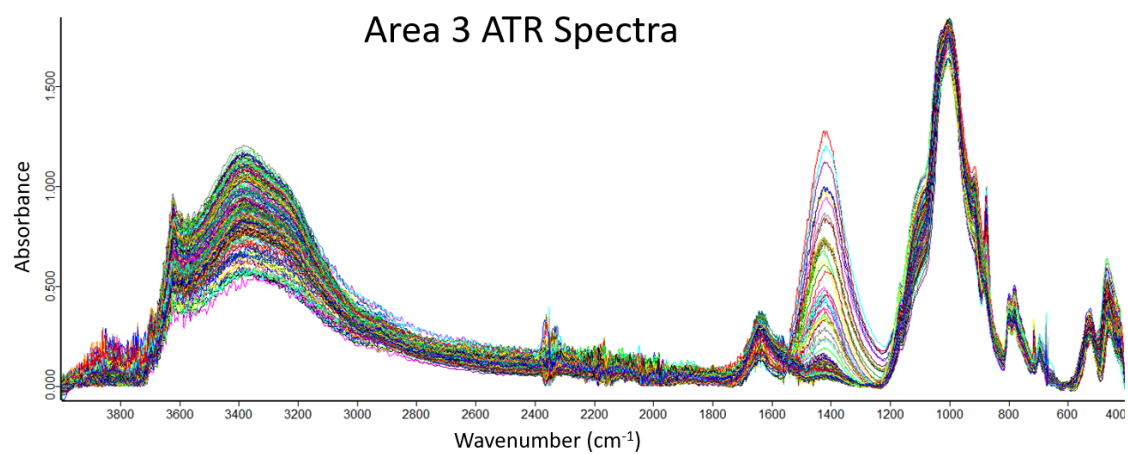


Figure 5: Area 3 ATR-FTIR Spectra Consisting of 20 Surface Samples and 20 Sub-surface Samples with 5 Replicates Each

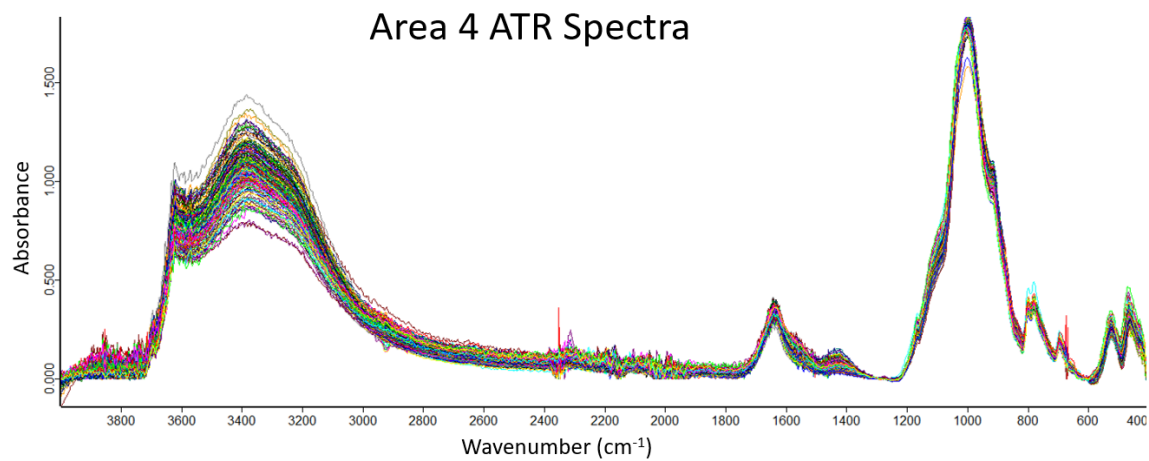


Figure 6: Area 4 ATR-FTIR Spectra Consisting of 20 Surface Samples and 20 Sub-surface Samples with 5 Replicates Each

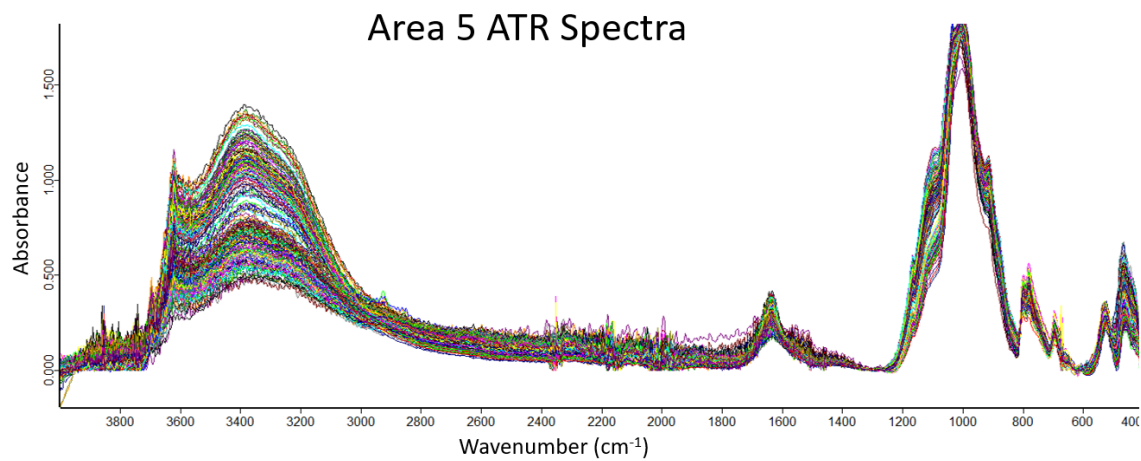


Figure 7: Area 5 ATR-FTIR Spectra Consisting of 20 Surface Samples and 20 Sub-surface Samples with 5 Replicates Each

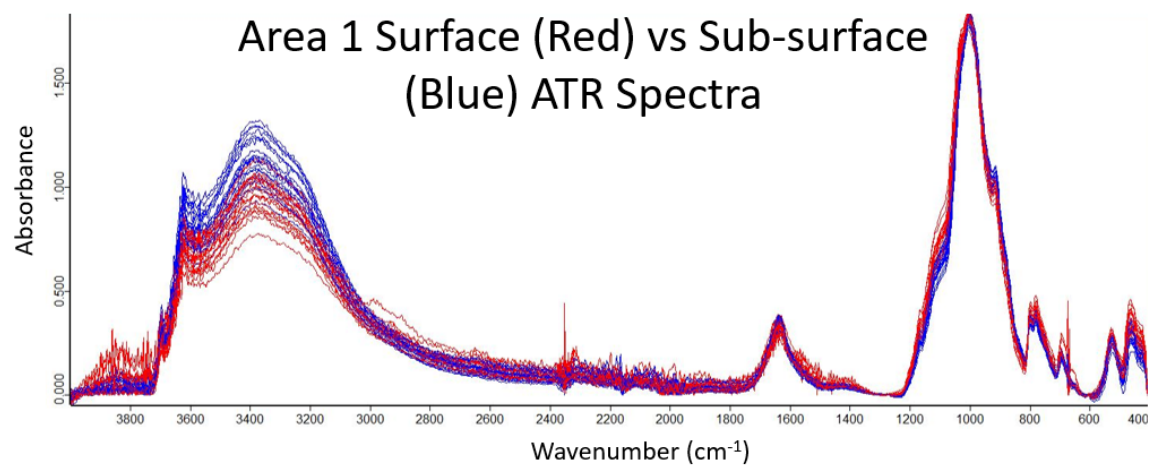


Figure 8: Area 1 ATR-FTIR Layer Spectra Consisting of 20 Surface Samples (red) and 20 Sub-surface Samples (blue)

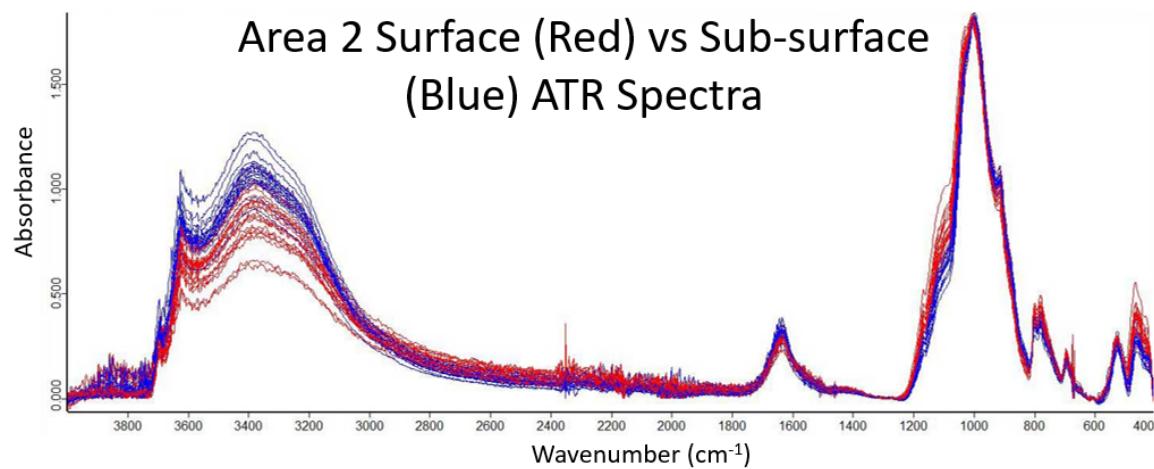


Figure 9: Area 2 ATR-FTIR Layer Spectra Consisting of 20 Surface Samples (red) and 20 Sub-surface Samples (blue)

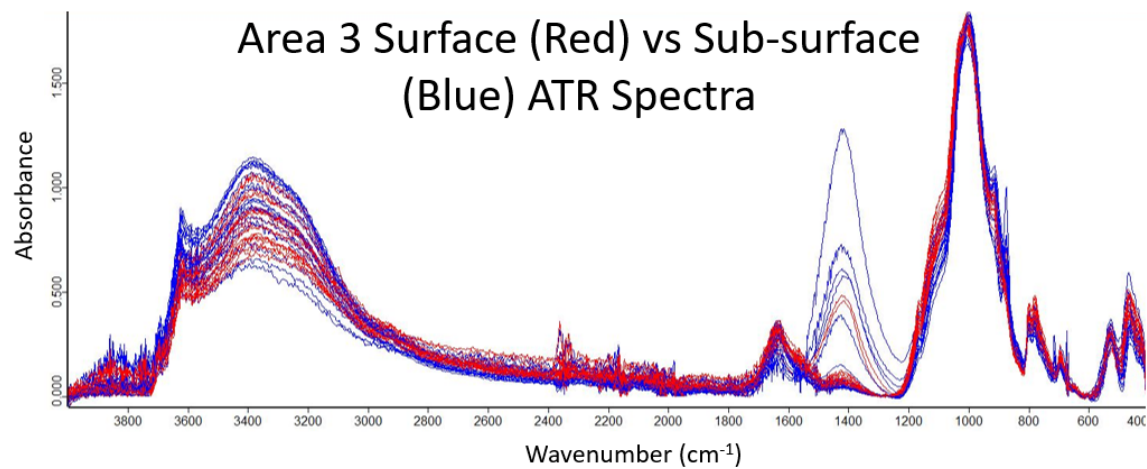


Figure 10: Area 3 ATR-FTIR Layer Spectra Consisting of 20 Surface Samples (red) and 20 Sub-surface Samples (blue)

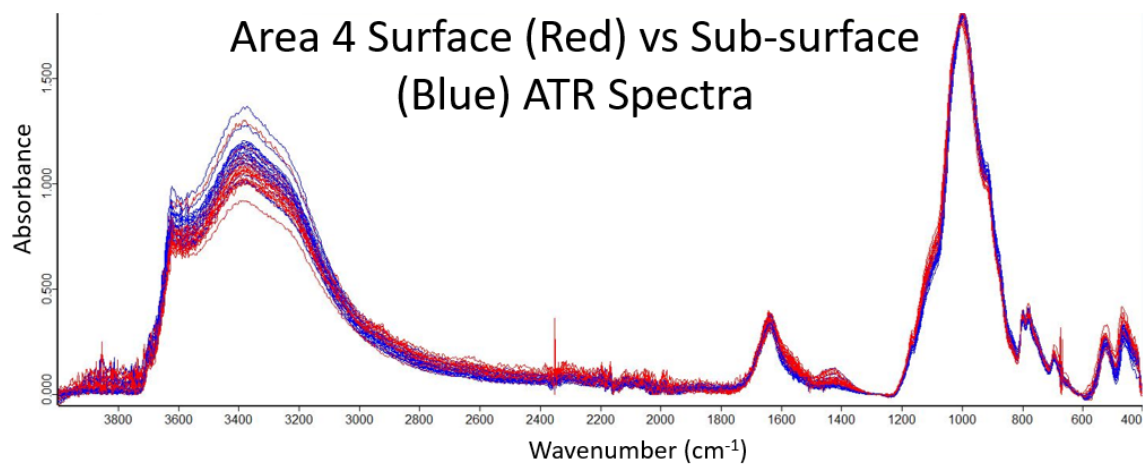


Figure 11: Area 4 ATR-FTIR Layer Spectra Consisting of 20 Surface Samples (red) and 20 Sub-surface Samples (blue)

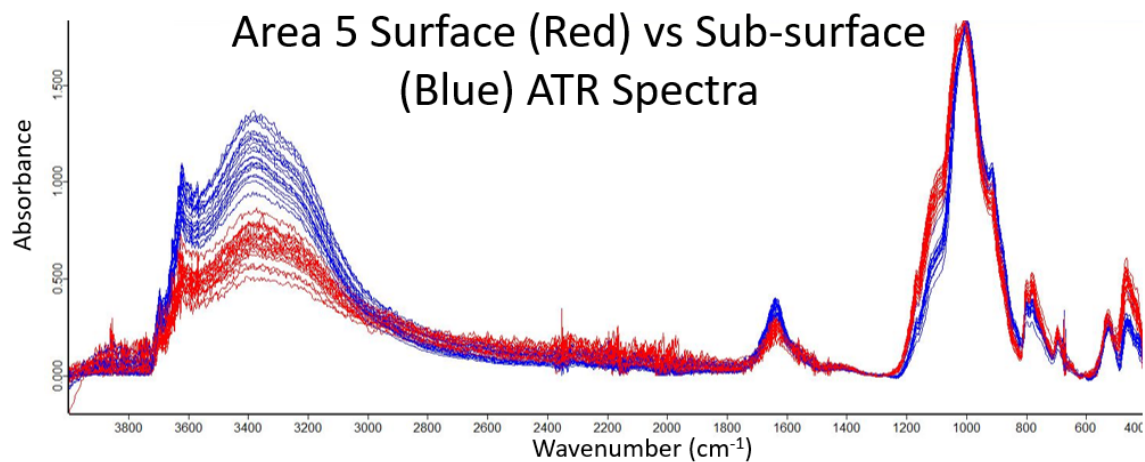


Figure 12: Area 5 ATR-FTIR Layer Spectra Consisting of 20 Surface Samples (red) and 20 Sub-surface Samples (blue)

Unknown 25 Air Dried vs Oven Dried Spectra

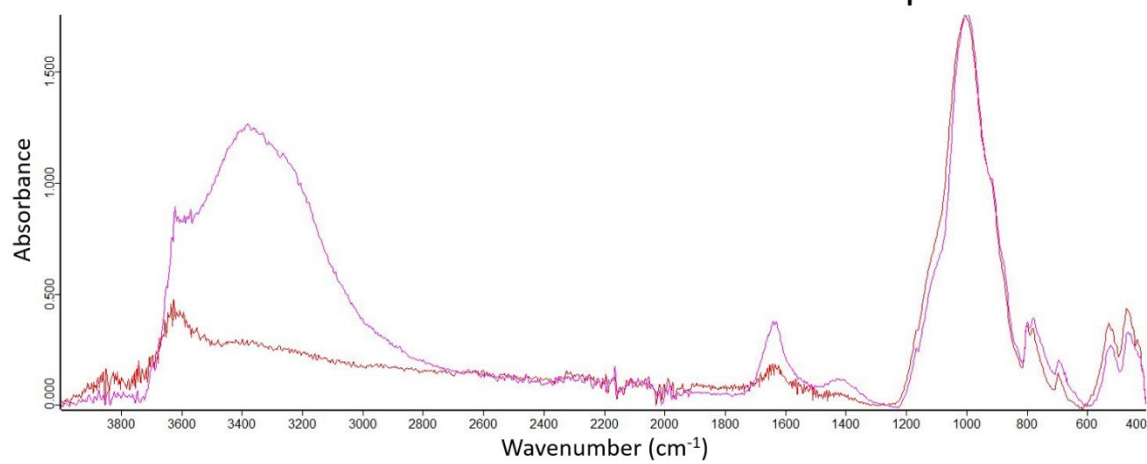


Figure 13: Unknown Sample 25 ATR-FTIR Spectra Air Dried (pink) Compared to Oven Dried (red)

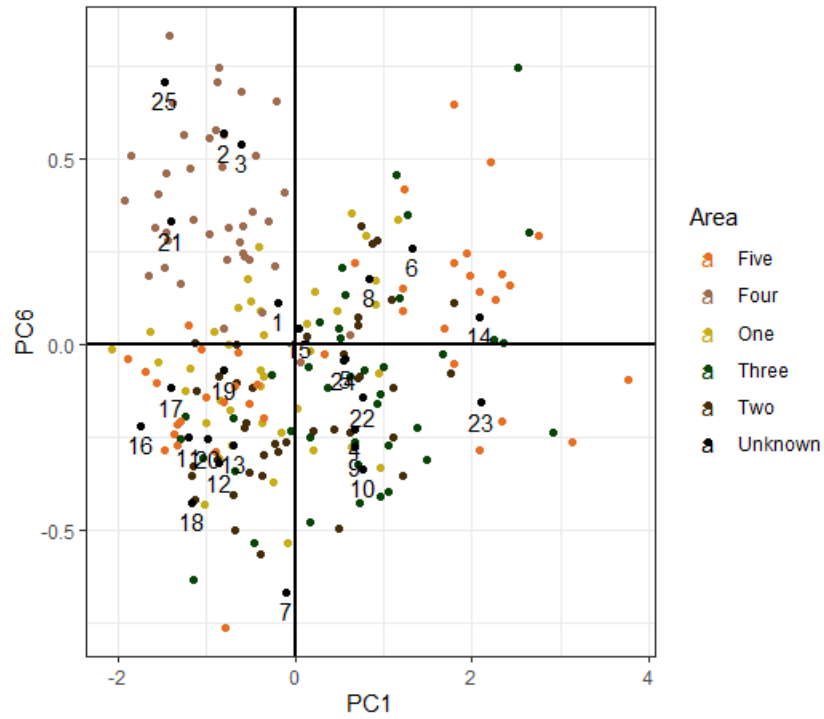


Figure 14: PCA Ordination Plot displaying PC1 and PC6 for Soil Area

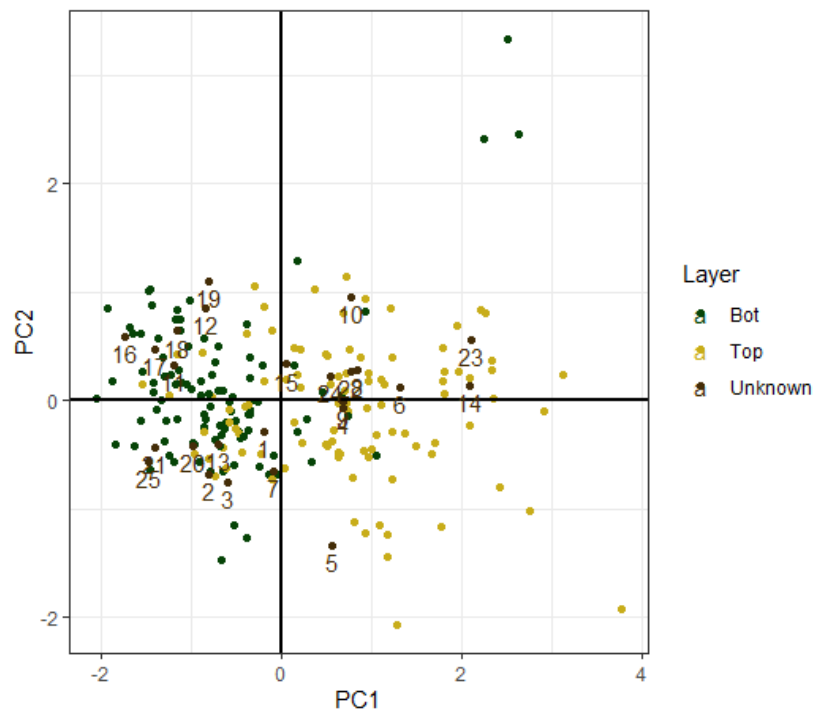


Figure 15: PCA Ordination Plot displaying PC1 and PC2 for Soil Layer

Table 1: Results of OPUS Spectra Search and PCA Compared to Actual Soil Origin

SAMPLE	SPECTRASEARCH TOP HIT	ACTUAL	PCA RESULTS
U-1	Area 1 top	Area 3 bot	Area 3 bot
U-2	Area 4 bot	Area 4 bot	Area 4 bot
U-3	Area 4 top	Area 4 top	Area 4 top
U-4	Area 1 top	Area 3 bot	Area 3 bot
U-5	Area 4 top	Area 4 top	Area 4 top
U-6	Area 5 top	Area 5 top	Area 5 top
U-7	Area 5 bot	Area 5 bot	Area 5 bot
U-8	Area 2 top	Area 2 top	Area 2 top
U-9	Area 2 top	Area 2 top	Area 2 top
U-10	Area 3 bot	Area 3 bot	Area 3 bot
U-11	Area 1 bot	Area 1 bot	Area 1 bot
U-12	Area 2 bot	Area 2 bot	Area 2 bot
U-13	Area 3 bot	Area 3 bot	Area 3 bot
U-14	Area 5 top	Area 5 top	Area 5 top
U-15	Area 2 top	Area 1 top	Area 1 top
U-16	Area 5 bot	Area 1 bot	Area 1 bot
U-17	Area 2 bot	Area 1 bot	Area 1 bot
U-18	Area 1 bot	Area 3 bot	Area 3 bot
U-19	Area 2 top	Area 2 top	Area 2 top
U-20	Area 5 bot	Area 1 bot	Area 1 bot
U-21	Area 4 bot	Area 4 bot	Area 4 bot
U-22	Area 1 top	Area 5 top	Area 5 top
U-23	Area 5 top	Area 5 top	Area 5 top
U-24	Area 2 top	Area 2 top	Area 2 top
U-25	Area 4 bot	Area 4 bot	Area 4 bot
CORRECT FOR TOP HIT=	68%		100%
CORRECT FOR TOP 5 HITS=	92%		NA

Table 2: Proposed Assignments for Peak Positions in the ATR-FTIR Spectra

Wavenumber (cm⁻¹)	Proposed Assignments	Characterization	References
3695	O-H stretching	Kaolinite	Vaculikova et al., Ojima
3623	O-H stretching	Kaolinite	Vaculikova et al., Ojima
3394	O-H stretching	Water Hydration	Salil et al., Anbalagan et al.
1632	H-O-H deformation	Water Hydration	Salil et al., Anbalagan et al.
1422	C-O stretching	Calcite	Gunasekaran et al.
1100	Asymmetric Si-O stretching	Quartz, Kaolinite	Vaculikova et al., Ojima
995	In-plane Si-O stretching	Kaolinite	Vaculikova et al.
911	O-H bending	Kaolinite	Vaculikova et al., Ojima
872	Asymmetric CO ₃ deformation	Calcite	Gunasekaran et al.
795	Si-O-Si symmetrical stretching	Quartz, Kaolinite	Vaculikova et al., Ojima
777	Si-O-Si symmetrical stretching	Quartz	Ojima
692	Si-O bending	Quartz, Kaolinite	Vaculikova et al., Ojima

Table 3: PCA Eigenvalues and Their Contribution to the Correlations

Initial Eigen Values			
Principal Components	Total	Proportion Explained	Cumulative %
1	855.9834	0.4903	0.4903
2	264.3147	0.1514	0.6416
3	171.35446	0.09814	0.73978
4	76.8405	0.04401	0.78379
5	62.98685	0.03607	0.81986
6	58.04543	0.03324	0.85311

Permission to Copy Statement

With my typed signature below, I, (Shelby Young), hereby submit this thesis/dissertation to Emporia State University as partial fulfillment of the requirements for an advanced degree. I agree that the Library of the University may make it available to use in accordance with its regulation governing materials of this type. I further agree that quoting, photocopying, digitizing or other reproduction of this document is allowed with proper attribution for private study, scholarship (including teaching) and research purposes of a nonprofit nature. No copying which involves potential financial gain will be allowed without written permission of the author. I also agree to permit the Graduate School at Emporia State University to digitize and place this thesis in the ESU institutional repository, and ProQuest Dissertations and Thesis database and in ProQuest's Dissertation Abstracts International.

Shelby Young

Typed Signature of Author

30MAY2020

Date

Testing the Use of Attenuated Total Reflectance Fourier Transform Infrared Spectroscopy for
Differentiating Forensic Soil Samples in Kansas

Title of Thesis